The Plant Cell, Vol. 13, 2257–2268, October 2001, www.plantcell.org © 2001 American Society of Plant Biologists

Plastid Division Is Driven by a Complex Mechanism That Involves Differential Transition of the Bacterial and Eukaryotic Division Rings

Shin-ya Miyagishima,[1] Manabu Takahara, Toshiyuki Mori, Haruko Kuroiwa, Tetsuya Higashiyama, and Tsuneyoshi Kuroiwa

Department of Biological Sciences, Graduate School of Science, University of Tokyo, Hongo, Tokyo 113-0033, Japan

During plastid division, two structures have been detected at the division site in separate analyses. The plastid-dividing ring can be detected by transmission electron microscopy as two (or three) electron-dense rings: an outer ring on the cytosolic face of the outer envelope, occasionally a middle ring in the intermembrane space, and an inner ring on the stromal face of the inner envelope. The FtsZ ring, which plays a central role in bacterial division, also is involved in plastid division and is believed to have descended to plastids from cyanobacterial endosymbiosis. The relationship between the two structures is not known, although there is discussion regarding whether they are identical. Biochemical and immunocytochemical investigations, using synchronized chloroplasts of the red alga *Cyanidioschyzon merolae*, showed that the plastid FtsZ ring is distinct and separable from the plastid-dividing ring. The FtsZ ring localizes in stroma and faces the inner plastid-dividing ring at the far side from the inner envelope. The FtsZ ring and the inner and outer plastid-dividing rings form in that order before plastid division. The FtsZ ring disappears at the late stage of constriction before dissociation of the plastid-dividing ring, when the constriction is still in progress. Our results suggest that the FtsZ ring–based system, which originated from a plastid ancestor, cyanobacteria, and the plastid-dividing ring–based system, which probably originated from host eukaryotic cells, form a complex and are involved in plastid division by distinct modes.

INTRODUCTION

Plastids are essential for the viability of all plants and function in photosynthetic carbon assimilation, nitrate and sulfate assimilation, and lipid and amino acid synthesis. Animals require the products of plastids for survival. It is widely believed that plastids and mitochondria arose from bacterial endosymbionts related to present cyanobacteria and α-proteobacteria, respectively (Gray, 1992). Although most of their genes have been transferred to the host nuclear genome, plastids and mitochondria have several features similar to those of bacteria. Both types of organelle have nucleoids and ribosomes and are never synthesized de novo. Their continuity is maintained by the division of preexisting organelles and their inheritance by daughter cells during cell division (reviewed by Kuroiwa, 1991).

The mechanism of plastid division has been analyzed by ultrastructural observation and, recently, by molecular genetic studies incorporating accumulated information about bacterial division. Ultrastructural studies established that plastids divide by constriction division (reviewed by Possingham and Lawrence, 1983; Leech and Pyke, 1988; Whatley, 1988) and showed that electron-dense ring structures encircling the constricted furrow of dividing plastids can be detected by transmission electron microscopy (reviewed by Kuroiwa et al., 1998). The ring structure, called the plastid-dividing ring (PD ring), was first identified on the cytosolic face of the outer envelope in a red alga (outer PD ring) (Mita et al., 1986). Subsequently, fine-section studies resolved the PD ring into two rings and identified the inner PD ring on the stromal face of the inner envelope in addition to the outer PD ring (Hashimoto, 1986). A few earlier studies reported structures in the constriction zone of plastids (Suzuki and Ueda, 1975; Chaly and Possingham, 1981; Leech et al., 1981), but, as described elsewhere in detail (Kuroiwa, 1989), their interpretation of the structure and location were incorrect. The outer and inner PD rings now have been detected in several lines of algae and land plants, and they are thought to be ubiquitous in plant cells (Tewinkel and Volkmann, 1987; Oross and Possingham, 1989; Duckett and Ligrone, 1993a, 1993b; summarized by Kuroiwa et al., 1998). In the red alga *Cyanidioschyzon merolae*, a middle PD ring also was identified in the intermembrane space (Miyagishima et al., 1998a). Observing the PD ring generally is difficult because, in most cases, plastids divide nonsynchronously and the PD rings are very small structures that are detected only in the final stage of division using good fixation techniques.

[1] To whom correspondence should be addressed. E-mail miyagi@biol.s.u-tokyo.ac.jp; fax 81-3-3814-1408.

We studied the unicellular red alga *C. merolae*, which contains a single chloroplast, mitochondrion, and nucleus. Its PD rings can be observed clearly just before the onset of constriction division. The division of each organelle is synchronized easily by a light/dark cycle (Suzuki et al., 1994). Previous ultrastructural studies have shown that the three PD rings of *C. merolae* behave differently throughout the plastid division cycle, suggesting that the proteins forming the rings differ (Miyagishima et al., 1998b, 1999a, 2001b). Recently, we succeeded in preparing the outer PD ring subfraction and revealed that it consists of a bundle of novel 5-nm filaments (Miyagishima et al., 2001a). The results suggest that the outer PD ring does not have a cyanobacterial origin but was newly created by the host cell, probably to regulate the division of the cyanobacterial endosymbiont. The components of the outer PD ring are under investigation, whereas the ultrastructure and components of the middle and inner PD rings are still unknown.

The discovery of a nucleus-encoded homolog of a key bacterial division protein, FtsZ, located in Arabidopsis plastids (Osteryoung and Vierling, 1995) has enabled further understanding of the molecular mechanism of plastid division. In bacteria, FtsZ forms a ring structure, called the Z ring, on the inner face of the cytoplasmic membrane at the division site. FtsZ assembles into filaments in a GTP-dependent manner in vitro and is a structural homolog of eukaryotic tubulin (reviewed by Bramhill, 1997; Rothfield et al., 1999). Several FtsZs have been isolated from algae and land plants, and most of them are very similar to their cyanobacterial counterpart (summarized by Osteryoung and Pyke, 1998; Pyke, 1999; Beech and Gilson, 2000; Osteryoung, 2000; Gilson and Beech, 2001). Two types of FtsZ (FtsZ1 and FtsZ2) have been found in higher plants, and it is reported that, unlike FtsZ1, which is imported into plastids (Osteryoung et al., 1998; Gaikwad et al., 2000), FtsZ2 does not contain a transit peptide and is not imported into chloroplasts in vitro (Osteryoung et al., 1998). Nevertheless, two FtsZs from the moss *Physcomitrella patens* related to higher plant FtsZ2 were transported into chloroplasts when tagged with green fluorescent protein (GFP) (Kiessling et al., 2000). Moreover, a lily (*Lilium longiflorum*) FtsZ from the FtsZ2 family (Mori and Tanaka, 2000) possesses a cleavable transit peptide and localizes inside the chloroplast (Mori et al., 2001). Recently, an open reading frame of Arabidopsis FtsZ2-1 was identified that was longer than that reported previously (the deduced N terminus of the protein is 81 amino acids longer than the previously reported open reading frame) (GenBank AF089738; Osteryoung and McAndrew, 2001). Therefore, higher plant FtsZ2, in addition to FtsZ1, probably functions inside plastids.

Disruption of *ftsZ* in *P. patens* (Strepp et al., 1998) and antisense repression of *FtsZ* in Arabidopsis (Osteryoung et al., 1998) blocked plastid division, suggesting that plant FtsZs are involved in plastid division. In addition, a nucleus-encoded homolog of MinD, which determines the division site in bacteria, also was shown to determine the division site of plastids (Colletti et al., 2000). These results suggest that a significant part of the bacterial division system was introduced by the cyanobacterial endosymbiont itself and was maintained by the plastid during evolution. As conclusive evidence of this notion, a recent immunofluorescence microscopic study showed that FtsZ forms a ring at the site of chloroplast division in higher plants (Vitha et al., 2001). This was also observed by immunoelectron microscopy (Mori et al., 2001). Before these reports, the experiment introducing GFP-tagged FtsZ in the moss showed FtsZ-containing cytoskeleton-like networks in chloroplasts (Kiessling et al., 2000). Nevertheless, as shown by Vitha et al. (2001), these probably were artifacts of excess amounts of GFP-tagged FtsZ. Although the PD ring could not be detected by the immunological method for electron microscopy, the lily Z ring was localized inside plastids at a location similar to that of the inner PD ring (Mori et al., 2001). The similar location of the two structures implies that they are identical. Nevertheless, because bacterial Z rings cannot be observed directly as electron-dense structures in thin sections, we believe that the electron-dense inner PD ring is distinct from the Z ring (Miyagishima et al., 2001a, 2001b). The relationship between these two structures must be clarified to relate the two lines of study for further understanding of plastid division.

This study provides biochemical and immunocytochemical evidence that the Z ring is distinct from the electron-dense inner PD ring. We reveal the spatiotemporal relationship between the Z and PD rings in *C. merolae*. We connect morphological and molecular genetic studies of plastid division and suggest that plastid division involves a two-mechanism complex: the Z ring of cyanobacterial origin and the PD ring probably from the host eukaryote.

RESULTS

The PD ring of *C. merolae* is composed of a 10- to 40-nm-thick outer ring on the cytoplasmic face of the outer envelope and a 5-nm-thick inner ring on the stromal face of the inner envelope, as observed in other plant species. A 2-nm-thick middle ring was detected in the intermembrane space in a fine section (Figures 1A to 1C; Miyagishima et al., 1998a). Similar to higher plants (Mori et al., 2001; Vitha et al., 2001), immunofluorescence microscopy showed that FtsZ formed a ring at the division site of chloroplasts in *C. merolae* (Figures 1D and 1E). Because several plant FtsZs are shown to be imported into plastids (Osteryoung and Vierling, 1995; Osteryoung et al., 1998; Gaikwad et al., 2000; Kiessling et al., 2000) and the lily Z ring was localized inside the chloroplast (Mori et al., 2001), the Z ring observed in this study was thought to be located at the stromal face of the inner envelope, as is the inner PD ring.

To determine whether the Z ring was identical to the inner PD ring, we compared the stability of the two structures using chloroplasts isolated from synchronized cells and pos-

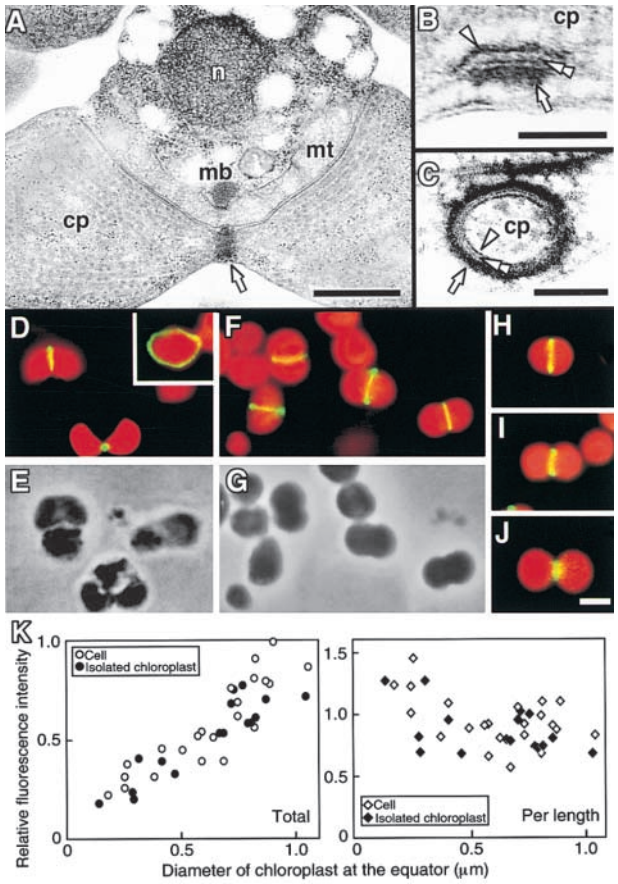

Figure 1. Micrographs of the PD and Z Rings in *C. merolae*.

(A) to **(C)** Electron micrographs of a dividing cell in which the PD ring is cut tangentially **(A)**. Magnified cross-sectional **(B)** and circumferential **(C)** views of the PD ring show that it consists of three rings.

(D) and **(E)** Immunofluorescence image of Z rings in dividing cells **(D)** and a phase-contrast image of the same field **(E)**. The inset shows a circumferential image of the Z ring. Green fluorescence indicates the localization of FtsZ, and red indicates the autofluorescence of chlorophyll on the thylakoid.

(F) and **(G)** Immunofluorescence image of Z rings in dividing chloroplasts isolated from a synchronous culture **(F)** and a phase-contrast image of the same field **(G)**.

(H) to **(J)** The Z ring in isolated chloroplasts at early **(H)**, middle **(I)**, and late stages of division **(J)**.

(K) Relative fluorescence intensity of fluorescein isothiocyanate labeling of the Z ring in whole cells (open circles and open diamonds) and isolated chloroplasts (closed circles and closed diamonds) plotted versus diameter of the chloroplast at the equator. The total intensity of the Z ring (left; open circles and closed circles) was converted to intensity per 1 μm (right; open diamonds and closed diamonds).

Arrows, arrowheads, and double arrowheads indicate the outer, inner, and middle PD rings, respectively. cp, chloroplast; mb, microbody; mt, mitochondrion; n, nucleus. Bar in **(A)** = 500 nm; bar in **(B)** = 50 nm; bar in **(C)** = 100 nm; bar in **(J)** = 1 μm for **(D)** to **(J)**.

sessing PD rings. Before the experiment, we confirmed that the conditions of medium and lower temperatures (known to destabilize tubulin-based structures) used for the isolation procedure did not destabilize the Z ring. Immunofluorescence microscopy showed that the isolated chloroplasts had Z rings as they do in vivo (Figures 1F to 1J). The fluorescence intensities of Z rings in isolated chloroplasts were almost the same as those in cells at every stage of division (Figures 1H to 1K), indicating that the FtsZ molecules involved in the Z ring were not affected by chloroplast isolation. The fact that lower temperatures did not destabilize in vivo FtsZ polymers, unlike their structural homologs, tubulin polymers, is consistent with results obtained for FtsZ polymers generated in vitro (Bramhill and Thompson, 1994).

The total fluorescence intensity of the Z ring decreased along with contraction (Figures 1H to 1K), as observed in lily (Mori et al., 2001), suggesting that the total number of FtsZ molecules that make up the ring decreases with contraction. The fluorescence intensity of the Z ring per length increased during contraction (Figures 1H to 1K), suggesting that the cross-sectional area of the ring increased. This change in the Z ring during contraction is similar to that of the inner PD ring determined previously by transmission electron microscopy (Miyagishima et al., 1999a).

The Z and Inner PD Rings Are Not Identical

Although information on the biochemical properties of the Z and inner PD rings was not available, the effect of several factors on tubulin polymers (summarized by Timasheff and Grisham, 1980) and the in vitro assembly of FtsZ into polymers (Bramhill and Thompson, 1994; Erickson et al., 1996; Mukherjee and Lutkenhaus, 1998, 1999; Lu et al., 2000) are well characterized. Referring to these studies, we examined the stability of the Z ring in situ under different conditions before comparing it with the inner PD ring.

Isolated chloroplasts were burst in different hypotonic media. The insoluble pellet containing membranes, and the supernatant containing stroma, were separated by centrifugation at 10,000*g*. FtsZ was detected by immunoblotting and in some cases by immunofluorescence microscopy. The majority of FtsZ molecules were detected in the supernatant of the sucrose-depleted chloroplast isolation medium (Figure 2A), indicating that the Z ring was disassembled or detached from the envelope and existed in the supernatant. When the supernatant was negatively stained and examined by transmission electron microscopy, no ring-like structures or large fragments were detected, although many small particles less than 40 nm were detected (data not shown). This result suggested that the Z ring was disassembled to small fragments or monomers in the medium.

We thought that the Z ring was disassembled by osmotic shock, thus bringing it into direct contact with destabilizing factors in the medium. Compared with media used to handle FtsZ or tubulin polymers, the chloroplast isolation medium

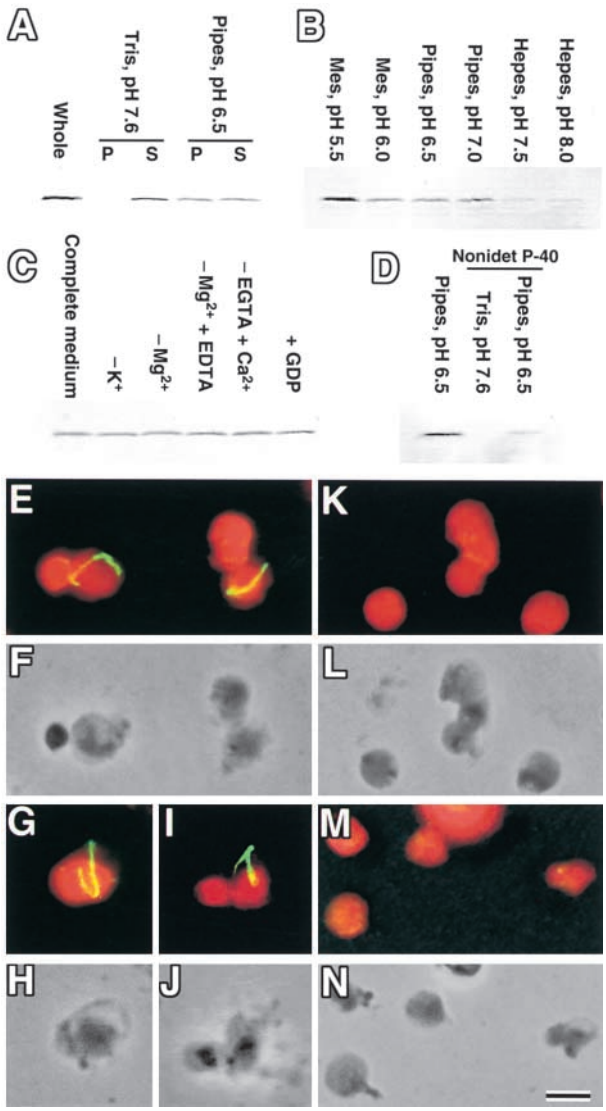

Figure 2. Effect of Several Factors on the Stability of the Z Ring.

(A) to **(D)** Isolated chloroplasts were burst by osmotic shock in hypotonic media and centrifuged, and FtsZ was detected by immunoblotting.
(A) Sucrose-depleted chloroplast isolation medium (pH 7.6) and the same medium in which Tris (pH 7.6) was replaced with Pipes (pH 6.5) were used, and the pellet (P) and supernatant (S) were analyzed. Untreated isolated chloroplasts also were analyzed (whole).
(B) Media buffered at various pH values were used, and the pellets were analyzed.
(C) Chemicals were depleted from (−) or added to (+) medium containing Pipes (pH 6.5), KCl, $MgCl_2$, and EGTA (complete medium), and the pellets were analyzed.
(D) Media buffered with Pipes (pH 6.5) or Tris (pH 7.6) with or without 0.1% Nonidet P-40 were used, and the pellets were analyzed.
(E) to **(N)** Immunofluorescence (**[E]**, **[G]**, **[I]**, **[K]**, and **[M]**) and phase contrast images (**[F]**, **[H]**, **[J]**, **[L]**, and **[N]**) of burst chloroplasts at pH 6.5 (**[E]** to **[J]**), pH 7.5 (**[K]** and **[L]**), and pH 5.5 (**[M]** and **[N]**) detecting the Z ring. **(F)**, **(H)**, **(J)**, **(L)**, and **(N)** are the same fields of view as **(E)**, **(G)**, **(I)**, **(K)**, and **(M)**, respectively. Bar in **(N)** = 1 μm for **(E)** to **(N)**.

differs only in pH; the former are at pH 6.0 to 7.0 (Erickson et al., 1996; Mukherjee and Lutkenhaus, 1998, 1999; Lu et al., 2000), and the latter is at pH 7.6. To test the possibility that the pH of the medium decomposed the Z ring, Tris (pH 7.6) was replaced with Pipes (pH 6.5); subsequently, half of the FtsZ molecules were pelleted (Figure 2A). Immunofluorescence showed that the fluorescence intensity of the Z ring did not diminish (Figures 2E to 2J), suggesting that the FtsZ detected in the supernatant at pH 6.5 was derived from stroma and was not involved in the Z ring in situ. The Z rings often remained at the edges of phase-contrast images in which the autofluorescence of thylakoids was absent, indicating that the ring adhered to the envelope membrane (Figures 2G to 2J). From these results, we concluded that the Z ring is stable at pH 6.5 but unstable at pH 7.6. This finding suggests that the Z ring is sensitive to pH.

Further pH studies showed that the Z ring was stable only at pH 6.0 to 7.0 and became destabilized at pH values less than 6.0 or greater than 7.0. At pH 7.5 or 8.0, the Z ring was absent in fluorescence microscopy (Figures 2K and 2L) and FtsZ protein was not detected in the pellet by immunoblotting (Figure 2B), indicating that the Z ring had been disassembled. At pH 5.5, the Z ring was absent (Figures 2M and 2N) but FtsZ protein was detected in the pellet and was more abundant than at pH 6.0 to 7.0 (Figure 2B), probably as a result of aggregation. These results involving Z rings in situ are similar to the in vitro results for polymers of FtsZ efficiently generated or maintained at approximately pH 6.5 (Mukherjee and Lutkenhaus, 1998, 1999). The depletion or addition of chemicals did not cause any significant changes in the amount of FtsZ pelleted after osmotic shock (Figure 2C), although the depletion of Mg^{2+} or the addition of Ca^{2+} destabilizes polymers of tubulin (Timasheff and Grisham, 1980). These results are consistent with the report that the removal of Mg^{2+} or the addition of Ca^{2+} did not destabilize FtsZ polymers in vitro but inhibited their turnover (Mukherjee and Lutkenhaus, 1999). The previously reported solubilization of FtsZ, but not the outer PD ring, by the nonionic detergent Nonidet P-40 (Miyagishima et al., 2001a) was not attributable to the pH of the medium used (pH 7.6), because a similar result was obtained at pH 6.5 (Figure 2D).

To compare the effect of pH on the inner PD and Z rings, chloroplasts burst at several pH values were examined by transmission electron microscopy. Treated chloroplasts were depleted of stroma but had envelopes and thylakoids, thus confirming that they had burst (Figures 3A and 3B). At pH 5.5 or 7.5, although the Z ring was absent by immunoflu-

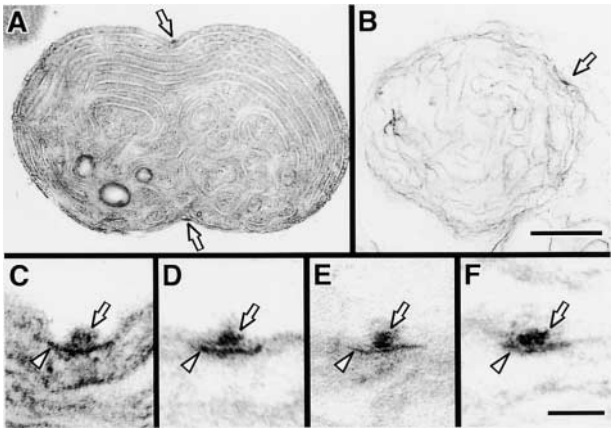

Figure 3. Effect of pH on the Stability of the PD Ring.

(A) and **(B)** Whole electron microscopic image of an isolated chloroplast before **(A)** and after **(B)** being burst in medium at pH 7.6.
(C) to **(F)** Magnified cross-sectional image of the PD ring before **(C)** and after being burst in medium at pH 5.5 **(D)**, 6.5 **(E)**, or 7.5 **(F)**.
Arrows and arrowheads indicate the outer and inner PD rings, respectively. Bar in **(B)** = 500 nm for **(A)** and **(B)**; bar in **(F)** = 50 nm for **(C)** to **(F)**.

orescence (Figure 2), both the outer and inner PD rings were observed (Figures 3D and 3F). The thickness and electron density of the outer and inner PD rings were no less than in chloroplasts before treatment (Figures 3C, 3D, and 3F). Furthermore, no structures around the PD ring were detected specifically at pH 6.5 (Figure 3E), whereas the Z ring was observed by immunofluorescence only at pH 6.5 (Figure 2). These results suggest that the Z ring is a structure that is distinct and separable from both the inner and the outer PD rings, and like the bacterial Z ring, the plastid Z ring is invisible in electron microscopic sections. This invisibility probably is the result of the poor contrast of the Z ring rather than the size of the Z ring, because the visible inner PD ring was 5 nm thick, which is approximately the size of one FtsZ molecule.

The Z, Inner PD, and Outer PD Rings Form in This Order

This conclusion raises the question of how the Z and PD rings are related to each other spatially and temporally. We previously showed that the inner PD ring forms first and then the middle and outer PD rings form at approximately the same time, before constriction of the division site (Miyagishima et al., 1998b). RNA gel blot analyses showed that transcripts of *ftsZ* accumulated specifically before chloroplast division in *C. merolae* (Takahara et al., 2000). The Z ring forms when constriction is not evident in *C. merolae* (Figure 1) and higher plants (Mori et al., 2001; Vitha et al., 2001). These results indicate that both the PD and Z rings form before plastid division. To clarify the temporal relationship of the PD and Z rings, the two rings were compared in synchronous culture around the onset of chloroplast division. In *C. merolae*, the shape of chloroplasts changed sequentially from acorn shaped to cup shaped to trapezoidal to dumbbell shaped (Figures 4A to 4D). In acorn- or cup-shaped chloroplasts, the PD ring was absent (Figure 4E; Miyagishima et al., 1998b). In trapezoidal chloroplasts, the inner PD ring formed first, followed by the middle and outer PD rings (Figure 4F; Miyagishima et al., 1998b). A portion of synchronous culture was harvested 2 hr before the onset of the second dark period (34 hr) and 0 and 2 hr after the onset of the second dark period (36 and 38 hr). At the first two time points, most of the chloroplasts were cup shaped, and at the last time point, some of the chloroplasts had become trapezoidal (Figures 4G to 4M). Immunofluorescence microscopy showed that the Z ring could be detected scarcely at 34 hr (Figures 4H and 4I) but had formed at 36 hr in ~30% of the chloroplasts (Figures 4J and 4K), indicating that the Z ring forms in cup-shaped chloroplasts from which the PD ring is absent (Figure 4E). At 38 hr, the Z ring was more evident (Figures 4L and 4M). These and previous results (Miyagishima et al., 1998b) show that the rings of dividing chloroplasts form in the following order: Z, inner PD, and outer PD rings.

The Inner PD Ring Is Located between the Z Ring and the Inner Envelope

To clarify the spatial relationship between the Z and the PD rings, we performed immunoelectron microscopy. Isolated chloroplasts were used rather than whole cells, because whole cells shrank during fixation and embedding in resin for immunoelectron microscopy, producing unclear images (data not shown). Fixation for immunoelectron microscopy usually resulted in lower contrast images of sections than electron microscopy only for structural observation. In fact, we could not obtain profiles of the PD ring in lily by immunoelectron microscopy when FtsZ was labeled with gold particles (Mori et al., 2001). Using *C. merolae* chloroplasts, in which the PD ring can be observed more clearly than in higher plants, we obtained profiles of both the PD and Z rings in the same section by immunoelectron microscopy (Figure 5). Gold labeling was concentrated at the stromal face of the envelope at the division site, and there was no signal on the outer PD ring (Figure 5A). In addition to dense labeling at the division site, gold particles also were dispersed around the chloroplast, except in the center nucleoid regions of the two daughter chloroplasts (Figure 5A). These dispersed labels were not observed with preimmune serum or the secondary antibody alone (data not shown). Thus, the label probably detected FtsZ molecules that were not involved in the Z ring.

This interpretation is consistent with the results of immunoblot analysis, which detected about half of the FtsZ molecules in the stromal fraction without decomposition of the Z ring

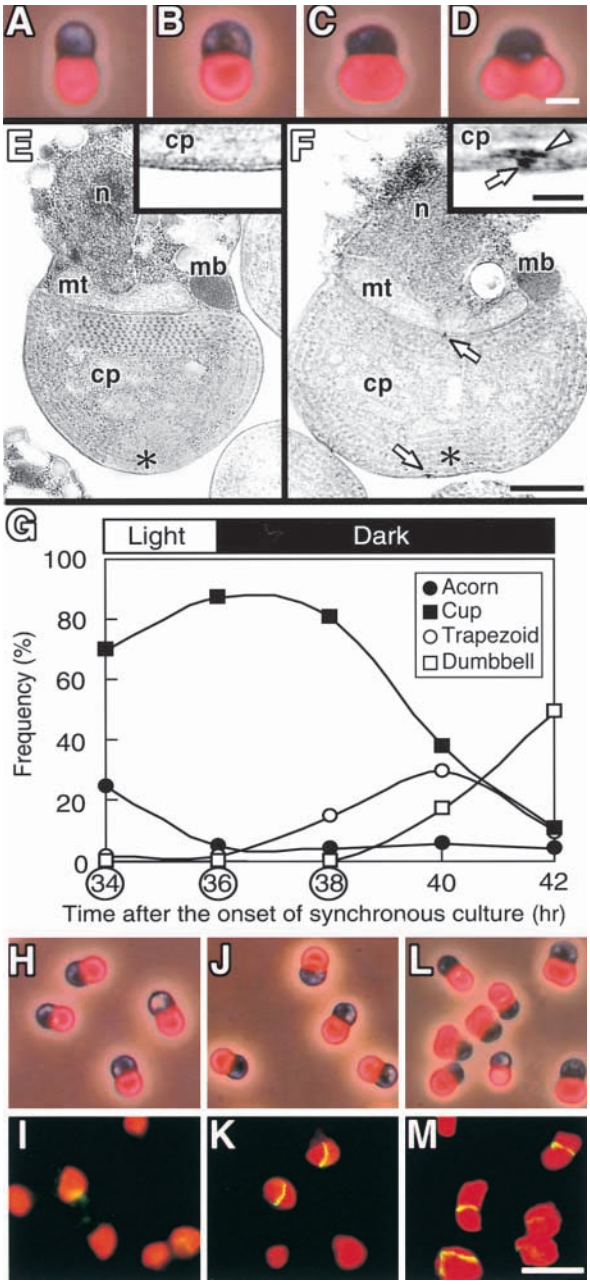

Figure 4. Timing of the Formation of the Z and PD Rings in Synchronous Culture.

(A) to **(D)** Autofluorescence of chloroplast/phase–contrast images showing the transition of chloroplast shape in *C. merolae* in the order acorn **(A)**, cup **(B)**, trapezoid **(C)**, and dumbbell **(D)**.

(E) and **(F)** Electron micrographs of cells with cup-shaped **(E)** or trapezoidal chloroplasts **(F)**. Magnified images of the regions indicated by asterisks are shown in the insets. Arrows and the arrowhead indicate the outer and inner PD rings, respectively. cp, chloroplast; mb, microbody; mt, mitochondrion; n, nucleus.

(G) Change in the frequency of cells containing acorn-shaped (closed circles), cup-shaped (closed squares), trapezoidal (open circles), and dumbbell-shaped (open squares) chloroplasts in synchronous culture.

(H) to **(M)** Autofluorescence of chloroplast/phase–contrast images without fixation of the synchronous culture at 34 hr **(H)**, 36 hr **(J)**, and 38 hr **(L)** and immunofluorescence micrographs showing the Z ring at 34 hr **(I)**, 36 hr **(K)**, and 38 hr **(M)**.

Bar in **(D)** = 1 μm for **(A)** to **(D)**; bar in **(F)** = 500 nm for **(E)** and **(F)**; bar in inset of **(F)** = 50 nm for insets of **(E)** and **(F)**; bar in **(M)** = 5 μm for **(H)** to **(M)**.

(Figure 2A). In sections cut along the division site, 10-nm gold particles were lined one or two deep, indicating that the Z ring is up to ~20 nm thick (Figures 5B and 5C). Comparison of the exact location of the Z ring with that of the PD ring required sections cut perpendicular to the PD ring; these resolved the outer and inner PD rings into two distinct rings. Gold particles touched the surface of the section, whereas the image of the section was obtained as a projection of all the material embedded in the section, which was ~70 nm thick in this study. Therefore, sections not perpendicular to the PD ring, which do not allow resolution of the outer and inner PD rings, cause a lag between the surface of the section and the image of the section, confusing the distance between structures and gold particles. In sections resolving the inner and outer PD rings, gold particles lined the stromal side of the inner PD ring (Figures 5D to 5F). Behind the gold particles, no electron-dense structures could be detected (Figures 5D to 5F). These results indicate that the Z ring is located as an invisible belt on the stromal side of the inner PD ring. Thus, the inner envelope, the inner PD ring, and the Z ring are stratified in this order toward the inside of the chloroplast. Together with the timing of formation (Figure 4), this finding suggests that the Z ring forms first, at a distance from the inner envelope; then the inner PD ring forms between the Z ring and the inner envelope.

The Z Ring and the Three PD Rings Behave Differently during Chloroplast Division

The results described above revealed that the Z ring and the three PD rings are distinct and form a complex at the site of plastid division. To further investigate how the four parts of the division complex (Z, inner PD, middle PD, and outer PD rings) behave during plastid division, sequential changes in the PD ring and the gold label for FtsZ were examined (Figures 5G to 5M). Dimensions of the PD rings and the region of gold labeling of the Z ring were measured in sections cutting the PD rings at the center perpendicular to the divisional plane, as described in detail in Methods and by Miyagishima et al. (1999a). These sections avoid overestimation of dimensions by cutting the rings at an angle. In some chloroplasts in which constriction was not evident and the PD ring was absent, a linear pattern of labeling indicat-

ing the Z ring was observed (Figure 5G), confirming that the Z ring forms before the PD ring (Figure 4). The region of gold particles widened with contraction, but it did not change in thickness (Figures 5G to 5J and 5M). The density of label did not change, and the deduced volume of the Z ring decreased with contraction (Figure 5G to 5J and 5M). This is in contrast to the outer PD ring, which widens and thickens while maintaining a constant volume during contraction (Miyagishima et al., 1999a; Figure 5M).

On the other hand, the mode of contraction of the Z ring was similar to changes observed for the inner and middle PD rings (Miyagishima et al., 1999a; Figure 5M). Widening, with reduction of the volume of the Z ring, is consistent with the results of immunofluorescence studies showing that the intensity of fluorescence per length increased but the total intensity decreased during contraction (Figure 1). Combined, the Z, middle, and inner PD rings contract with a loss of components. A notable difference is that the label localizing the Z ring is wider than the inner PD ring (Figures 5I, 5J, and 5M). At the late stage of division, when the constriction was still in progress, the FtsZ label was absent in the region encircled by the PD ring and was dispersed toward the two daughter chloroplasts (Figure 5K). This finding indicates that the Z ring disappears before the inner and outer PD rings during the late stage of chloroplast division. At the completion of division, the inner and middle PD rings disappeared, whereas the outer PD ring was left between the daughter chloroplasts (Miyagishima et al., 2001b; Figure 5L) and there was a reduced amount of dispersed gold label around the division site (Figure 5L). These and previous observations (Miyagishima et al., 2001b) indicate that the Z ring disappears and then the inner and middle PD rings disappear about the same time before the completion of division, unlike the outer PD ring, which remains in the cytosol after division.

In summary, the present and previous observations (Miyagishima et al., 1998b, 2001b) indicate that the Z and the PD rings form a complex structure by the contact between the Z ring and the inner PD rings and that the Z, inner PD, and outer PD rings form and disappear in this order. In addition to the biochemical study in vitro (Figure 2), Figures 5G and 5K show that the Z ring is separable from the inner PD ring in vivo.

DISCUSSION

Although the Z and PD rings were localized previously to the plastid division site, their relationship was not clear, because the two structures had not been studied together in the same experiment. This study showed that the two structures are distinct; they form at different times and locations, although the Z ring faces the inner PD ring. In contrast to the PD ring, but like the bacterial Z ring, the plastid Z ring was invisible in electron microscopy sections, probably because of poor contrast. Previously, we showed that the outer PD ring consists of novel 5-nm filaments distinct from the FtsZ filament (Miyagishima et al., 2001a). This study showed that the inner PD ring (and the middle PD ring in *C. merolae*) also is distinct from the Z ring.

Extensive molecular genetic studies of cell division in *Escherichia coli* have identified nine proteins involved in the division apparatus, namely FtsA, FtsI, FtsK, FtsL, FtsN, FtsQ, FtsW, FtsZ, and ZipA (summarized by Bramhill, 1997; Rothfield et al., 1999). Two of these proteins (FtsZ and FtsI) are encoded in the genome of the cyanobacterium *Synechocystis* strain PCC6803. Arabidopsis possesses only FtsZ in its genome. Although it is possible that cyanobacteria have unique proteins involved in the division apparatus that are absent in *E. coli*, no electron-dense structures like the PD ring have been observed at the division sites in cyanobacteria, as seen in other bacteria. Thus, it is highly probable that both the inner and outer PD rings (and the middle PD ring of *C. merolae*) are not identical to any parts involved in the bacterial division machinery. Therefore, we suggest that plastid division involves the cooperation of two systems. One is based on the Z ring, which originated from the cyanobacterial endosymbiont itself, and the other is based on the PD ring, which probably was added by the host cell after endosymbiosis.

Identification of the components of the PD ring is needed to provide convincing evidence for this suggestion and to clarify whether the PD rings were created de novo by the host eukaryotic cell or evolved from bacterial proteins or structures with modifications. Chloroplast division that retains the system of bacterial division is in contrast to mitochondrial division. Although mitochondrial FtsZs have been reported in some unicellular algae (Beech et al., 2000; reviewed by Beech and Gilson, 2000; Takahara et al., 2000; Gilson and Beech, 2001), they are absent in higher plants, fungi, and animals. It has been suggested that the mitochondria of most organisms divide by a system including dynamin-related GTPase that is newly created by the host eukaryotic cell (Bleazard et al., 1999; Labrousse et al., 1999; reviewed by Erickson, 2000; Margolin, 2000; Osteryoung, 2000). Plastids retain the bacterial division system, but this retention is partial. The loss of bacterial division proteins, other than FtsZ, and acquisition of the PD ring may have resulted in the loss of cell walls and the acquisition of an outer envelope in plastids. Some proteins involved in the bacterial division apparatus are thought to act in the periplasm, and one (FtsI) acts in peptide glycan synthesis (Bramhill, 1997; Rothfield et al., 1999). The outer PD ring may have evolved to pinch the plastid from the outside, thus replacing cell wall ingrowth at the division site, which occurs in bacteria.

On the basis of this and previous studies, the system based on the Z and PD rings for plastid division was compared with the system for bacterial division (Bramhill, 1997; Rothfield et al., 1999) (Figure 6). As in bacteria, the Z ring forms first at the expected site of division under the direction of the division site determining factor MinD. Although sequences homologous with *minC* have not been identified

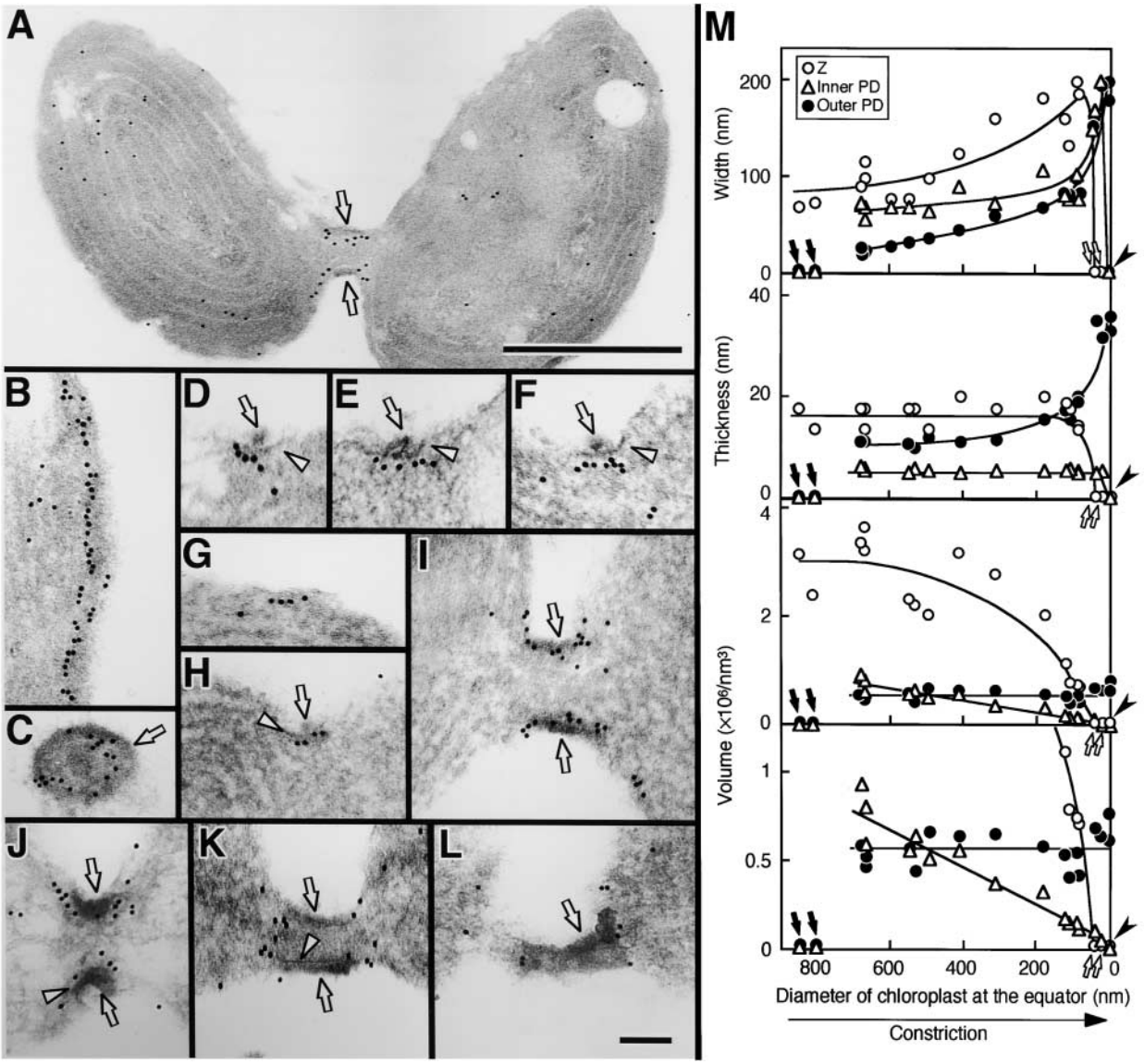

Figure 5. Immunoelectron Micrographs Showing the Localization and Change in Shape of the Z and PD Rings during Contraction.

FtsZ was labeled with gold particles.

(A) Whole image of an isolated dividing chloroplast.

(B) and **(C)** Sections cut along the chloroplast division site in the early **(B)** and late **(C)** stages of division.

(D) to **(F)** Sections cut perpendicular to the PD ring, in which the outer and inner PD rings are resolved into two distinct rings.

(G) to **(L)** Sections showing sequential change in the PD ring and the label for the FtsZ protein.

(M) Change in the width, thickness, and deduced volume of the region of gold particles labeling the Z ring (open circles), inner PD ring (open triangles), and outer PD ring (closed circles). The stage of division progresses from left to right. Because the diameter of the chloroplast at the equator decreases linearly with time (Miyagishima et al., 1999a), the *x* axis provides a relative time axis.

Arrows and arrowheads in **(A)** to **(L)** indicate the outer and inner PD rings, respectively. In **(M)**, closed arrows show points at which the Z ring has formed but the inner and outer PD rings have not yet formed, as in **(G)**; open arrows show points at which the Z ring was absent, unlike the inner and outer PD rings, as in **(K)**; closed arrowheads show points at which only the outer ring was present, as in **(L)**. Bar in **(A)** = 500 nm; bar in **(L)** = 100 nm for **(B)** to **(L)**.

in any algae and plants, *minE* encoded at least in plastid genomes of some algal species (reviewed by Osteryoung and McAndrew, 2001), and it was shown that MinD is involved in the determination of the plastid division site in Arabidopsis (Colletti et al., 2000). After Z ring formation, bacterial and plastid division follow separate processes. In bacteria, other division proteins are recruited to the division site in an FtsZ-dependent manner and septation starts (Bramhill, 1997; Rothfield et al., 1999). These proteins are absent in plastids, in which the inner PD ring forms between the Z ring and the inner envelope. Finally, the outer PD ring (and the middle PD ring in *C. merolae*) forms and constriction starts (Miyagishima et al., 1998b).

The proposed order of assembly of the PD rings relative to the Z ring is based on the formation of visually detectable electron-dense structures. Although accurate determination regarding individual components requires immunological detection, as performed for the Z ring, and it is possible that undetectable small rings have already formed before they become detectable in size, we used transmission electron microscopy to detect the inner PD ring at 5 nm in thickness (the thickness is constant during contraction) and the outer PD ring at 10 nm in thickness (the thickness increases during contraction) before constriction (Miyagishima et al., 1998b; Figures 1, 4, and 5). Because the thicknesses correspond to one or two protein molecules, the absence of the electron-dense structure in this case probably means that components of the rings are absent or dispersed even if they have been recruited on the membrane. Regarding the outer PD ring, an ultrastructural study at still higher resolution showed that it consists of filaments 5 nm in diameter in which proteins are spaced 4.8 nm apart (Miyagishima et al., 2001a).

This study localized the Z ring to beneath the inner PD ring at the far side of the inner envelope (Figure 5). This observation is consistent with the observation that loss of the Z ring at pH 5.5 or 7.5 did not detach the inner PD ring from the inner envelope (Figure 3). Nevertheless, the fact that the Z ring forms before the inner PD ring (Figure 4) raises the question of how the Z ring forms without direct contact with the envelope. Two possibilities are proposed: either the edges of the Z ring face the envelope, or long linker proteins form between the Z ring and the envelope, forming a space in which the 5-nm-thick inner PD ring is formed. The former proposal is based on the observation that the Z ring is wider than the inner PD ring (Figure 5). Regarding the latter proposal, ZipA, an integral membrane protein linking the Z ring to the membrane in *E. coli*, has a 300–amino acid proline/glutamine-rich domain that is predicted to form a long, rigid structure in the cytoplasm (Hale and de Boer, 1997; Erickson, 2001). ZipA is absent from the Arabidopsis genome, but a long linker such as ZipA may be involved in plastid division.

Although profiles of bacterial and plastid Z rings in vivo have not been obtained directly, profiles of the Z ring at several stages of chloroplast division obtained by immunoelectron microscopy using synchronized preparations provide information about its morphology and changes during contraction (Figure 6). The Z ring in plastids is belt shaped, less than 20 nm thick, and probably faces the inner PD ring directly. The antibody detected FtsZ proteins that are not involved in the Z ring (Figures 2A and 5A). FtsZ proteins are lost from the ring during contraction (Figures 1H to 1K, 5G to 5J, and 5M), and the Z ring is disassembled completely, before both the PD ring and the completion of division (Figure 5K). The fact that the density of gold label of the Z ring did not change in thin sections during constriction (Figures 5G to 5J) weakens the possibility of the reduction of fluorescent label (Figure 1) as a result of biochemical change of the Z ring during constriction. Although the Z ring and the two (or three) PD rings form a complex, their behavior during plastid division differs. This implies that the three (or four)

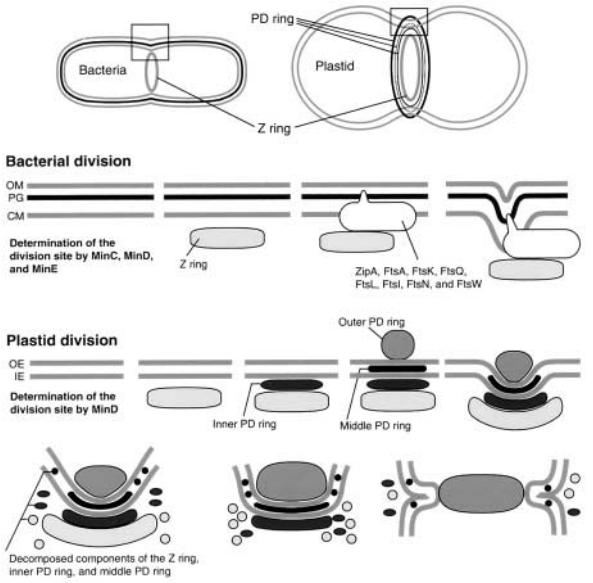

Figure 6. Comparison of the Division Machinery between Bacteria and Plastids and a Model of the Machinery of Plastid Division.

To illustrate the bacterial division machinery, the division complex characterized in *E. coli* is used. Of these proteins, MinC, MinD, MinE, FtsZ, and FtsI are found in the genome sequence of the cyanobacterium *Synechocystis* PCC6803. In bacterial division, MinC, MinD, and MinE determine the division site and FtsZ is first recruited at the expected division site. Other components of the division complex (ZipA, FtsA, FtsK, FtsQ, FtsL, FtsI, FtsN, and FtsW) are then recruited in a Z ring–dependent manner, and septum formation starts. In plastid division, at least MinD is involved in determining the division site. After the formation of the Z ring, the inner PD ring forms between the Z ring and the inner envelope. Finally, the outer PD ring (and the middle PD ring in *C. merolae*) forms and constriction starts. The Z and inner (and middle) PD rings decompose as they contract, whereas the outer PD ring contracts without loss of components. At the late stage of division, the Z and inner (and middle) PD rings disappear in that order. Finally, the outer PD ring pinches off the plastid and remains in the cytosol. CM, cytoplasmic membrane; IE, inner envelope; OE, outer envelope; OM, outer membrane; PG, peptide glycan.

rings have distinct roles. That the Z ring forms before the PD ring, and that contraction starts after the formation of the PD ring, suggest that the Z ring functions as scaffolding in plastid division, as suggested for bacterial division (Bramhill, 1997; Rothfield et al., 1999).

The fact that the Z ring also exists during contraction implies that it also plays a role that is not as clear as its role in bacterial division. Because the Z ring disappears at the late stage of chloroplast division, when constriction is still in progress (Figure 5K), it is suggested that the function of the Z ring during contraction is restricted to the earlier stage of constriction. The Z, inner PD, and middle PD rings disappear before the completion of division and thus do not become obstacles to membrane fusion. At the last phase of division, the outer PD ring probably functions in the final pinching off of the chloroplast.

To further reveal the structure and function of the Z and PD ring complex, identification of the components of the PD ring and direct ultrastructural observation of the Z ring are needed. The components of the PD ring are under investigation by fractionation of the PD ring (Miyagishima et al., 2001a). Regarding the structure of the Z ring, in vitro studies showed that FtsZ assembles into protofilaments and that the filament further forms the protofilament sheets, tubules, and mini rings depending on the medium condition (summarized by Lu et al., 2000). However, it is not known what kind of polymers FtsZ formed in vivo. The linear arrangement of FtsZ labeling on cross-sections by immunoelectron microscopy (Figure 5) supports the suggestion that the Z ring must be based on the protofilament sheets (Erickson et al., 1996). To obtain direct profiles of the Z ring requires electron microscopic techniques other than sectioning, (e.g., negative staining or freeze fracture). To use these techniques, the Z ring should be roughly fractionated. We showed that the Z ring was stable in medium at pH 6.5 and at lower temperatures (Figure 2); the use of similar media will reveal the profile of the Z ring and its biochemical interaction with the PD ring. This study showed that the Z ring dissociates at pH values greater than 7.0 (Figure 2). At present, however, it is unclear how the Z ring was stabilized in stroma, where the pH is approximately 8.0 in the light and more than 7.0 even in the dark (Heldt et al., 1973). One possibility is that some mechanism protects the Z ring from the stromal pH and that this mechanism was disrupted in the hypotonic medium at low ionic strength.

METHODS

Synchronization and Isolation of Dividing Chloroplasts of *Cyanidioschyzon merolae*

C. merolae strain 10D-14 (Toda et al., 1998) was cultured in Allen's medium. For synchronization, the cells were subcultured to $<1 \times 10^7$ cells/mL and subjected to a 12-hr-light/12-hr-dark cycle at 45°C (Suzuki et al., 1994). Dividing chloroplasts were isolated from the synchronized culture during the second dark period as described previously (Miyagishima et al., 1999c). Isolated chloroplasts suspended in isolation medium (20 mM Tris, pH 7.6, 5 mM $MgCl_2$, 5 mM KCl, 5 mM EGTA, and 300 mM sucrose) were kept on ice until use. Total protein concentrations from chloroplast fractions were measured with a protein assay kit (Bio-Rad).

Treatment of Z Rings in Isolated Chloroplasts with Various Media and Immunoblot Analysis Using Anti-FtsZ Antibody

Isolated chloroplasts containing 1 mg of protein were collected by centrifugation at 800*g* for 5 min at 4°C, burst in 1 mL of hypotonic media, and held on ice for 1 hr. The hypotonic media contained 5 mM KCl, 5 mM $MgCl_2$, 5 mM EGTA, and 100 μg/mL DNaseI (D4527; Sigma) in 20 mM Tris, Mes, Pipes, or Hepes buffered with NaOH at the pH values indicated in Results. DNaseI was added to avoid aggregation caused by the chromatin of chloroplast nucleoids. The effects of media chemicals on the stability of the Z ring were examined by the depletion or addition of chemicals. EDTA, $CaCl_2$, and GDP were added at concentrations of 5 mM. When $MgCl_2$ was depleted, the sample was initially treated with DNaseI in medium containing $MgCl_2$ and then was pelleted and treated with $MgCl_2$-depleted medium. The insoluble membrane fraction of burst chloroplasts was pelleted by centrifugation at 10,000*g* for 15 min at 4°C and washed with the same medium. The soluble fraction was concentrated and desalted in a Centricon-30 (30-kD cutoff; Millipore, Bedford, MA) with 50 mM Tris, pH 6.8. Soluble and insoluble fractions obtained from chloroplasts containing 0.1 mg of protein were immunoblotted with anti-CmFtsZ2 mouse antibody (Takahara et al., 2000) as described elsewhere (Miyagishima et al., 2001a).

Fluorescence and Electron Microscopy

For fluorescence microscopy, unfixed cells were examined under a phase-contrast/epifluorescence microscope (BHS-RFC; Olympus, Tokyo, Japan). The autofluorescence of chloroplasts was observed with green light excitation. Whole cells were observed by transmission electron microscopy after rapid freezing/freeze substitution (Miyagishima et al., 1999b). Isolated chloroplasts and the membrane pellet described above were fixed in 1% glutaraldehyde, postfixed with 1% OsO_4, and embedded in Spurr's resin as described (Miyagishima et al., 2001a). Thin sections were examined under an electron microscope (model JEM-1200EX; JEOL, Akishima, Tokyo, Japan).

Immunofluorescence and Immunoelectron Microscopy Using Anti-FtsZ Antibody

Pellets of cells, isolated chloroplasts, and the membrane fraction of chloroplasts were fixed in 3% (w/v) paraformaldehyde dissolved in 50 mM Pipes, pH 6.8, 10 mM EGTA, 5 mM $MgSO_4$, and 0.15 M sucrose for 1 hr at room temperature according to a fixation method for microtubules (Tanaka, 1991). After fixation, samples were washed twice with PBS. For immunofluorescence microscopy, samples were affixed to cover slips coated with poly-D-lysine (M_r 15,000 to 30,000; Sigma) and squashed beneath slide glasses. After being treated with 0.05% Triton X-100 in PBS for 15 min, the cover slips were blocked with 5% BSA in PBS for 30 min at 37°C. Then the cover slips were exposed to anti-CmFtsZ2 mouse antibody (1:100 dilution) for 2 hr at 37°C. After further washing with 1% BSA in PBS for 30 min and

blocking with 5% BSA in PBS for 30 min, the samples were labeled with fluorescein sheep anti-mouse IgG conjugate (1:200 dilution; Cappel, Durham, NC) for 2 hr at 37°C. After washing with 1% BSA in PBS for 30 min, the samples were mounted in antifade (Slowfade; Molecular Probes, Eugene, OR). The fluorescence intensity of the Z ring labeled by fluorescein isothiocyanate was measured with a chilled charge-coupled device camera (C5810; Hamamatsu Photonics, Hamamatsu, Japan) and IPLab Spectrum software (Solution Systems, Funabashi, Japan).

For immunoelectron microscopy, samples fixed as described above were embedded in LR White resin (London Resin Co., London, UK) and thin sections were treated according to the immunogold method of Osafune et al. (1990). Anti-CmFtsZ2 mouse antibody (1:100 dilution) and 10-nm gold goat anti-mouse conjugate (1:80 dilution; Zymed, San Francisco, CA) were used as primary and secondary antibodies, respectively. All measurement of the PD and Z rings followed Miyagishima et al. (1999a) and was performed only in serial thin sections cutting chloroplasts perpendicularly to the equator. The diameter of the chloroplast at the equator was measured at the middle in total serial sections containing an individual chloroplast. The width and thickness of the PD rings and the region of accumulated gold labeling detecting the Z ring were measured at the same sections or sections adjacent to where the diameter was measured. These sections cut the PD rings perpendicularly. The measurement of the PD ring was performed on high-contrast, enlarged photographs of sections at a magnification of ×200,000. The measurement of gold labeling was performed on moderate-contrast photographs at the same magnification. The total volumes of the rings were calculated from their width, thickness, and diameter, taking the division site as a circle.

ACKNOWLEDGMENTS

This work was supported by Research Fellowship 10148 to S.M. from the Japanese Society for the Promotion of Science for Young Scientists and by Grant Nos. 13206011, 12446222, and 12874111 to T.K. from the Ministry of Education, Science, and Culture of Japan and from the Program for the Promotion of Basic Research Activities for Innovative Biosciences.

Received May 11, 2001; accepted July 31, 2001.

REFERENCES

Beech, P.L., and Gilson, P.R. (2000). FtsZ and organelle division in protists. Protist **151,** 11–16.

Beech, P.L., Nheu, T., Schultz, T., Herbert, S., Lithgow, T., Gilson, P.R., and McFadden, G.I. (2000). Mitochondrial FtsZ in a chromophyte alga. Science **287,** 1276–1279.

Bleazard, W., McCaffery, J.M., King, E.J., Bale, S., Mozdy, A., Tieu, Q., Nunnari, J., and Shaw, J.M. (1999). The dynamin-related GTPase Dnm1 regulates mitochondrial fission in yeast. Nat. Cell Biol. **1,** 298–304.

Bramhill, D. (1997). Bacterial cell division. Annu. Rev. Cell Dev. Biol. **13,** 395–424.

Bramhill, D., and Thompson, C.M. (1994). GTP-dependent polymerization of *Escherichia coli* FtsZ protein to form tubules. Proc. Natl. Acad. Sci. USA **91,** 5813–5817.

Chaly, N., and Possingham, J.V. (1981). Structure of constricted proplastids in meristematic plant tissue. Biol. Cell **41,** 203–210.

Colletti, K.S., Tattersall, E.A., Pyke, K.A., Froelich, J.E., Stokes, K.D., and Osteryoung, K.W. (2000). A homologue of the bacterial division site-determining factor MinD mediates placement of the chloroplast division apparatus. Curr. Biol. **10,** 507–516.

Duckett, J.G., and Ligrone, R. (1993a). Plastid-dividing rings in the liverwort *Odontoschisma denudatum* (Mart) Dum. (Jungermanniales, Hepaticae). G. Bot. Ital. **127,** 318–319.

Duckett, J.G., and Ligrone, R. (1993b). Plastid-dividing rings in ferns. Ann. Bot. **72,** 619–627.

Erickson, H.P. (2000). Dynamin and FtsZ: Missing links in mitochondrial and bacterial division. J. Cell Biol. **148,** 1103–1105.

Erickson, H.P. (2001). The FtsZ protofilament and attachment of ZipA: Structural constraints on the FtsZ power stroke. Curr. Opin. Cell Biol. **13,** 55–60.

Erickson, H.P., Taylor, D.W., Taylor, K.A., and Bramhill, D. (1996). Bacterial cell division protein FtsZ assembles into protofilament sheets and minirings, structural homologs of tubulin polymers. Proc. Natl. Acad. Sci. USA **93,** 519–523.

Gaikwad, A., Babbarwal, V., Pant, V., and Mukherjee, S.K. (2000). Pea chloroplast FtsZ can form multimers and correct the thermosensitive defect of an *Escherichia coli ftsZ* mutant. Mol. Gen. Genet. **263,** 213–221.

Gilson, P.R., and Beech, P.L. (2001). Cell division protein FtsZ: Running rings around bacteria, chloroplasts and mitochondria. Res. Microbiol. **152,** 3–10.

Gray, M.W. (1992). The endosymbiont hypothesis revisited. Int. Rev. Cytol. **141,** 233–357.

Hale, C.A., and de Boer, P.A.J. (1997). Direct binding of FtsZ to ZipA, an essential component of the septal ring structure that mediates cell division in *E. coli*. Cell **88,** 175–185.

Hashimoto, H. (1986). Double-ring structure around the constricting neck of dividing plastids of *Avena sativa*. Protoplasma **135,** 166–172.

Heldt, H.W., Werdan, K., Milovancev, M., and Geller, G. (1973). Alkalization of the chloroplast stroma caused by light dependent proton flux into the thylakoid space. Biochim. Biophys. Acta **314,** 224–241.

Kiessling, J., Kruse, S., Rensing, S.A., Harter, K., Decker, E.L., and Reski, R. (2000). Visualization of a cytoskeleton-like FtsZ network in chloroplasts. J. Cell Biol. **151,** 945–950.

Kuroiwa, T. (1989). The nuclei of cellular organelles and the formation of daughter organelles by the "plastid-dividing ring." Bot. Mag. **102,** 291–329.

Kuroiwa, T. (1991). The replication, differentiation, and inheritance of plastids with emphasis on the concept of organelle nuclei. Int. Rev. Cytol. **128,** 1–62.

Kuroiwa, T., Kuroiwa, H., Sakai, A., Takahashi, H., Toda, K., and Itoh, R. (1998). The division apparatus of plastids and mitochondria. Int. Rev. Cytol. **181,** 1–41.

Labrousse, A.M., Zappaterra, M.D., Rude, D.A., and van der Bliek, A.M. (1999). *C. elegans* dynamin-related protein DRP-1 controls severing of the mitochondrial outer membrane. Mol. Cell **4,** 815–826.

Leech, R.M., and Pyke, K.A. (1988). Chloroplast division in higher plants with particular reference to wheat. In The Division and Segregation of Organelles, S.A. Boffey and D. Lloyd, eds (Cambridge, UK: Cambridge University Press), pp. 39–62.

Leech, R.M., Thomson, W.W., and Platt-Aloika, K.A. (1981). Observations on the mechanism of chloroplast division in higher plants. New Phytol. **87,** 1–9.

Lu, C., Reedy, M., and Erickson, H.P. (2000). Straight and curved conformations of FtsZ are regulated by GTP hydrolysis. J. Bacteriol. **182,** 164–170.

Margolin, W. (2000). Organelle division: Self-assembling GTPases caught in the middle. Curr. Biol. **10,** 328–330.

Mita, T., Kanbe, T., Tanaka, K., and Kuroiwa, T. (1986). A ring structure around the dividing plane of the *Cyanidium caldarium* chloroplast. Protoplasma **130,** 211–213.

Miyagishima, S., Itoh, R., Toda, K., Takahashi, H., Kuroiwa, H., and Kuroiwa, T. (1998a). Identification of a triple ring structure involved in plastid division in the primitive red alga *Cyanidioschyzon merolae*. J. Electron Microsc. **47,** 269–272.

Miyagishima, S., Itoh, R., Toda, K., Takahashi, H., Kuroiwa, H., and Kuroiwa, T. (1998b). Orderly formation of the double ring structures for plastid and mitochondrial division in the unicellular red alga *Cyanidioschyzon merolae*. Planta **206,** 551–560.

Miyagishima, S., Itoh, R., Toda, K., Kuroiwa, H., and Kuroiwa, T. (1999a). Real-time analyses of chloroplast and mitochondrial division and differences in the behavior of their dividing rings during contraction. Planta **207,** 343–353.

Miyagishima, S., Itoh, R., Toda, K., Kuroiwa, H., Nishimura, M., and Kuroiwa, T. (1999b). Microbody proliferation and segregation cycle in the single-microbody alga *Cyanidioschyzon merolae*. Planta **208,** 326–336.

Miyagishima, S., Itoh, R., Aita, S., Kuroiwa, H., and Kuroiwa, T. (1999c). Isolation of dividing chloroplasts with intact plastid-dividing rings from a synchronous culture of the unicellular red alga *Cyanidioschyzon merolae*. Planta **209,** 371–375.

Miyagishima, S., Takahara, M., and Kuroiwa, T. (2001a). Novel filaments 5 nm in diameter constitute the cytosolic ring of the plastid division apparatus. Plant Cell **13,** 707–721.

Miyagishima, S., Kuroiwa, H., and Kuroiwa, T. (2001b). The timing and manner of disassembly of the apparatuses for chloroplast and mitochondrial division in the red alga *Cyanidioschyzon merolae*. Planta **212,** 517–528.

Mori, T., and Tanaka, I. (2000). Isolation of the *ftsZ* gene from plastid-deficient generative cells of *Lilium longiflorum*. Protoplasma **214,** 57–64.

Mori, T., Kuroiwa, H., Takahara, M., Miyagishima, S., and Kuroiwa, T. (2001). Visualization of an FtsZ ring in chloroplasts of *Lilium longiflorum* leaves. Plant Cell Physiol. **42,** 555–559.

Mukherjee, A., and Lutkenhaus, J. (1998). Dynamic assembly of FtsZ regulated by GTP hydrolysis. EMBO J. **17,** 462–469.

Mukherjee, A., and Lutkenhaus, J. (1999). Analysis of FtsZ assembly by light scattering and determination of the role of divalent metal cations. J. Bacteriol. **181,** 823–832.

Oross, J.W., and Possingham, J.V. (1989). Ultrastructural features of the constricted region of dividing plastids. Protoplasma **150,** 131–138.

Osafune, T., Schiff, J.A., and Hase, E. (1990). Immunogold localization of LHCP II apoprotein in the Golgi of *Euglena*. Cell Struct. Funct. **15,** 99–105.

Osteryoung, K.W. (2000). Organelle fission: Crossing the evolutionary divide. Plant Physiol. **123,** 1213–1216.

Osteryoung, K.W., and McAndrew, R.S. (2001). The plastid division machine. Annu. Rev. Plant Physiol. Plant Mol. Biol. **52,** 315–333.

Osteryoung, K.W., and Pyke, K.A. (1998). Plastid division: Evidence for a prokaryotically derived mechanism. Curr. Opin. Plant Biol. **1,** 475–479.

Osteryoung, K.W., and Vierling, E. (1995). Conserved cell and organelle division. Nature **376,** 473–474.

Osteryoung, K.W., Stokes, K.D., Rutherford, S.M., Percival, A.L., and Lee, W.Y. (1998). Chloroplast division in higher plants requires members of two functionally divergent gene families with homology to bacterial *ftsZ*. Plant Cell **10,** 1991–2004.

Possingham, J.V., and Lawrence, M.E. (1983). Controls to plastid division. Int. Rev. Cytol. **84,** 1–56.

Pyke, K.A. (1999). Plastid division and development. Plant Cell **11,** 549–556.

Rothfield, L., Justice, S., and Garcia-Lara, J. (1999). Bacterial cell division. Annu. Rev. Genet. **33,** 423–448.

Strepp, R., Scholz, S., Kruse, S., Speth, V., and Reski, R. (1998). Plant molecular gene knockout reveals a role in plastid division for the homolog of the bacterial cell division protein FtsZ, an ancestral tubulin. Proc. Natl. Acad. Sci. USA **95,** 4368–4373.

Suzuki, K., and Ueda, R. (1975). Electron microscope observations on plastid division in root meristematic cells of *Pisum sativum* L. Bot. Mag. **88,** 319–321.

Suzuki, K., Ehara, T., Osafune, T., Kuroiwa, H., Kawano, S., and Kuroiwa, T. (1994). Behavior of mitochondria, chloroplasts and their nuclei during the mitotic cycle in the ultramicroalga *Cyanidioschyzon merolae*. Eur. J. Cell Biol. **63,** 280–288.

Takahara, M., Takahashi, H., Matsunaga, S., Miyagishima, S., Sakai, A., Kawano, S., and Kuroiwa, T. (2000). A putative mitochondrial *ftsZ* gene is encoded in the unicellular primitive red alga *Cyanidioschyzon merolae*. Mol. Gen. Genet. **264,** 452–460.

Tanaka, I. (1991). Microtubule-determined plastid distribution during microsporogenesis in *Lilium longiflorum*. J. Cell Sci. **99,** 21–31.

Tewinkel, M., and Volkmann, D. (1987). Observations on dividing plastids in the protonema of the moss *Funaria hygrometrica* Sibth: Arrangement of microtubules and filaments. Planta **172,** 309–320.

Timasheff, S.N., and Grisham, L.M. (1980). In vitro assembly of cytoplasmic microtubules. Annu. Rev. Biochem. **49,** 565–591.

Toda, K., Takano, H., Miyagishima, S., Kuroiwa, H., and Kuroiwa, T. (1998). Characterization of a chloroplast isoform of serine acetyltransferase from the thermo-acidophilic red alga *Cyanidioschyzon merolae*. Biochim. Biophys. Acta **1403,** 72–84.

Vitha, S., McAndrew, R.S., and Osteryoung, K.W. (2001). FtsZ ring formation at the chloroplast division site in plants. J. Cell Biol. **153,** 111–119.

Whatley, J.M. (1988). Mechanism and morphology of plastid division. In The Division and Segregation of Organelles, S.A. Boffey and D. Lloyd, eds (Cambridge, UK: Cambridge University Press), pp. 63–83.